

Monitoring water transparency of a hypertrophic lake (the Albufera of València) using multitemporal Sentinel-2 satellite images

Xavier Sòria-Perpinyà^{1,*}, Esther Patricia Urrego¹, Marcela Pereira-Sandoval¹, Antonio Ruiz-Verdú¹, Juan M. Soria², Jesús Delegido¹, Eduardo Vicente² and José Moreno¹

¹ Image Processing Laboratory, Universitat de València. C/ Catedrático José Beltrán Martínez, 2. 46980, Paterna, València.

² Cavanilles Institute of Biodiversity and Evolutionary Biology (ICBiBE). Universitat de València. C/ Catedrático José Beltrán Martínez, 2. 46980, Paterna, València.

* Corresponding author: javier.soria-perpina@uv.es

Received: 31/10/18

Accepted: 01/08/19

ABSTRACT

Monitoring water transparency of a hypertrophic lake (the Albufera of València) using multitemporal Sentinel-2 satellite images

The Albufera of València has been a hypertrophic lake since the 1970s. Extensive efforts to revert the system to a clear water state, such as wastewater treatment and green filters construction, have not yielded the desired results; Albufera is still qualified as “bad” according to the Spanish Water Framework Directive implementation. Currently, the lake requires constant monitoring, and water transparency, measured by Secchi disc depth (SDD), is a key parameter for evaluating water quality. Remote sensing offers substantial advantages over traditional monitoring methods such as SDD because it allows the quality of the surface waters to be continuously monitored. This work aimed to calibrate and validate an algorithm for SDD retrieval from Sentinel-2 (S2) (A and B) satellites with multispectral instrument (MSI) sensors (13 bands) from 404 nm to 2200 nm, spatial resolutions of 10, 20 and 60 m and a temporal frequency of 5 days (revisit at the equator)-values previously unattainable from open access images. The study was carried out with images from 2016 and 2017; only 40 of the 81 images of the Albufera captured by the S2 satellites could be used, mainly due to the presence of clouds. Once the images were downloaded, they were processed using SNAP 5 software. Images were then atmospherically corrected using the Sen2Cor tool, and the lake’s SDD was estimated using the developed algorithm. The estimated SDD data were validated against field samples; a total of 20 sampling campaigns were carried out to measure the SDD, and 114 samples were taken. Chlorophyll *a* concentrations from each sample point were also measured to allow for better data interpretation; hydrological, precipitation and wind data were also collected. The algorithm model’s calibration showed its robustness with an R^2 of 0.673 using 79 samples. Validation of the algorithm’s accuracy using 35 samples produced a low root mean squared error of 0.06 m, indicating a perfect fit between the predicted and observed data. Interpretation of thematic maps showed that SDD temporal variations follow an annual bimodal pattern where the increase of SDD is determined by a significant increase in water renewal. The retrieval algorithm to estimate the SDD from S2 satellite images is accurate and appropriate to use within a protocol whose main purpose is to monitor the ecological status of the Albufera of València.

Key words: water quality, water management, Secchi disk, remote sensing, Sentinel-2

RESUMEN

Seguimiento de la transparencia del agua de un lago hipertrófico (Albufera de València) utilizando imágenes multitemporales de Sentinel-2

Desde los años 70, la Albufera de Valencia es un lago hipertrófico, y a pesar de los esfuerzos para revertir el sistema a un estado de aguas claras, como el tratamiento de aguas residuales y la construcción de filtros verdes, estos no han dado los resultados esperados, clasificándose aún como malo según la implementación de la Directiva Marco del Agua en la legislación española. Actualmente el lago requiere un monitoreo constante y la transparencia del agua, como profundidad del disco

*Secchi (SDD), es un parámetro clave para el seguimiento de la calidad del agua. La teledetección ofrece ventajas sustanciales sobre los métodos tradicionales de monitoreo, siendo una herramienta óptima para el monitoreo continuo del estado de calidad de las aguas superficiales. El objetivo es calibrar y validar un algoritmo para la estimación de la SDD a partir de Sentinel-2 (A y B), con el sensor MSI, multiespectral (13 bandas) de 404 nm a 2200 nm, una resolución espacial de 10, 20 y 60 m y una frecuencia temporal de 5 días (revisita en el Ecuador), valores impensables en imágenes de libre acceso. De las 81 imágenes tomadas por el satélite entre 2016 y 2017, sólo se pudieron utilizar 40 imágenes debido a la presencia de nubes. Se utilizó el software SNAP 5 para el procesamiento, utilizando la herramienta Sen2Cor para la corrección atmosférica y el algoritmo desarrollado para estimar la SDD del lago. Para la validación con muestras de campo, se llevaron a cabo 20 campañas de muestreo, tomando 114 medidas de la SDD. También se midió la concentración de clorofila *a* en cada punto de muestreo y se recogieron datos hidrológicos, de precipitación y viento. La calibración muestra su robustez con un R^2 de 0.673 utilizando 79 muestras. Los resultados de la validación utilizando 35 muestras son muy buenos, con un RMSE de 0.06 m, mostrando la precisión del algoritmo. De la interpretación de los mapas temáticos, extrajimos que la variación temporal de la SDD sigue un patrón bimodal anual, donde el aumento de la SDD viene determinada por un aumento significativo de la renovación del agua. El algoritmo desarrollado para estimar la SDD a partir de imágenes S2 es preciso y apropiado para su uso dentro de un protocolo para monitorizar el estado ecológico del lago.*

Palabras clave: *calidad del agua, gestión hídrica, disco de Secchi, teledetección, Sentinel-2*

INTRODUCTION

Light is one of the physical factors with the greatest influence on the structure and biological behavior of water bodies (Weyl, 1970; Wetzel, 1975; Owen, 1985). Light in the wavelengths of 400-700 nm (Photosynthetically Active Radiation) is crucial in quality and quantity for the photosynthesis of benthic and pelagic primary producers (Kirk, 1994). Therefore, light is a fundamental factor in the ecology of aquatic ecosystems (Wetzel, 2001) and water quality applications (Esteves, 1998; Effler *et al.*, 2005). Water transparency is a key parameter for monitoring water quality and can be used to detect anthropogenic impact due to dredging, erosion and eutrophication (Iannuzzi *et al.*, 1996; Ruffink, 1998; Wang *et al.*, 1999).

In oceanography and limnology, transparency measured with a Secchi disk (SD) is used to estimate light extinction in water (French *et al.*, 1982). The SD is the most widely used conventional method for measuring water column transparency. The distance traveled by the disk until its disappearance is called the Secchi disc depth (SDD). The SDD provides information that relates directly to human perceptions of lake water quality, and it is a reasonable indicator of trophic conditions (algal abundance) except in very highly colored lakes with low chlorophyll *a* concentration [Chl-*a*] or non-algal turbidity (e.g.,

clay, calcium carbonate; Brezonik *et al.*, 2005).

The SDD is inversely proportional to the average amount of inorganic and organic material in the water (Preisendorfer, 1986). There is a direct positive correlation between reflectance in the red spectral region and the gross particulate load (which induces particulate scattering); therefore, when water clarity as measured by SDD decreases, brightness in the red spectral region usually increases (Matthews, 2011). In this sense, remote sensing offers substantial advantages over traditional monitoring methods, mainly because of its synoptic coverage and the temporal consistency of the data, which has the potential to provide crucial information on inland and near-coastal transitional waters in countries where conventional water-quality monitoring programs are either lacking or unsatisfactory (Navalgund *et al.*, 2007).

Remotely sensed data have been used to estimate water quality parameters with moderate to high accuracy since the early 1980s (Lathrop, 1985; Schneider & Mauser, 1996). A review of the latest studies investigating optically complex waters commonly known as case-2 (Matthews, 2011; Dörnhöfer & Oppelt, 2016; Gholizadeh *et al.*, 2016) shows that the principal studied parameters are [Chl-*a*], suspended particulate matter and the CDOM (colored dissolved organic matter) is increasing. SDD is less studied and has mainly been done using Landsat and Medium Resolution Imaging Spectrometer (MERIS) satellites.

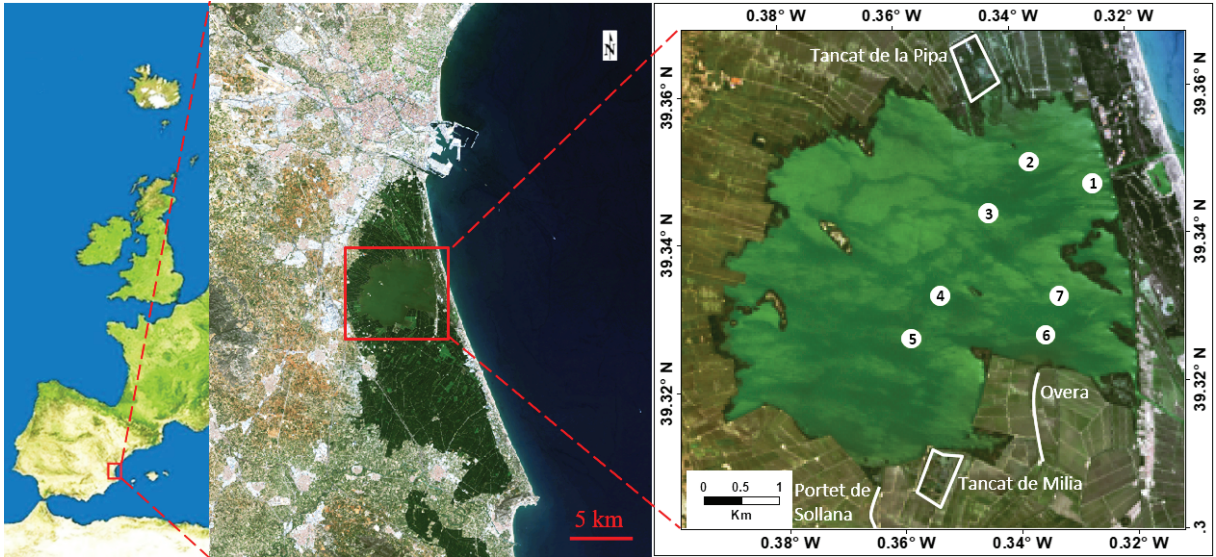


Figure 1. Study site, Albufera of València and sampling locations. *Lugar de estudio, Albufera de València y puntos de muestreo.*

Few studies of the Albufera of València have estimated water transparency using remote sensing. Several examples are Doña *et al.* in 2011 and 2014 using Band 2 (520–600 nm) of a Thematic Mapper (TM) sensor on board a Landsat 5 satellite to estimate water transparency as SDD. TM sensors has a spatial resolution of 30 m and a revisit time of 16 days, while Sentinel-2 (S2) (A and B) satellites, the new generation of European Earth-observation satellites, has spatial resolutions of 10, 20 and 60 m and a revisit time of 5 days (at the equator). Ten-meter resolution has not been available in open-access images until recently, making the S2 an excellent tool for intensifying studies on water bodies. Thus, recent studies based on SDD have used S2 satellites in either a semi-analytical scheme (Rodrigues *et al.*, 2017) or an empirical method (Batur & Maktav, 2019; Bonansea *et al.*, 2019).

The aim of this study was investigate the temporal and spatial evolution of transparency as an SDD measure throughout years 2016 and 2017, in order to calibrate and validate an algorithm for S2 images obtained with the MSI reflectance sensor and not with simulated Sentinel-2 imagery and develop an effective method for the multitemporal study of the Albufera of València, Spain.

MATERIALS AND METHODS

Study area

Albufera of València is a Mediterranean coastal oligohaline (1-2 ‰) shallow lake (1-3 m) situated 15 km south of the city of València (Spain) (Fig. 1). It is the largest natural lake of the Iberian Peninsula, with a surface area of 23.2 km², a volume of 23 x 10⁶ m³ and a water renewal rate of about ten times per year. It is considered a hypertrophic lake, with average annual [Chl-*a*] levels of 167 µg/L (4-322 µg/L), an SDD of 0.34 m (0.18-1.0 m), total phosphorus of 155 µg/L (41-247 µg/L) and total nitrogen of 3.9 mg/L (1.8-6.6 mg/L) (Onandia *et al.*, 2015).

Eutrophication began in the Albufera lake of València in the 1960s, when the basin and its surrounding experienced a great urban and industrial development and the urban and industrial wastewaters discharges went directly into the brooks and irrigation channels and on to the lake. The system shifted from a clear into a turbid stable state, which was consolidated by the virtual disappearance of macrophytes in the early 1970s (Vicente & Miracle, 1992). Despite all efforts to reverse the quality of Albufera lake to a clear

water state, such as wastewater treatment and green filter construction around the lake, it remains eutrophic and is classified as bad according to the Spanish Water Framework Directive (WFD) implementation. Furthermore, the pressure on this system is increasing due to population growth within its area of influence (waters with a high load of nutrients) and the effects of climate change (temperature rise, reduction of precipitation and increase in evaporation) (Sòria-Perpinyà *et al.*, 2019).

Albufera of València's hydrology is regulated according to the needs of surrounding agricultural lands (mainly rice paddies) by the local water council. Water inflow is via irrigation channels and outflow is to the Mediterranean Sea via sluice gates located at three outlet canals according to an annual pattern summarized in Miracle and Sahuquillo (2002) and detailed in Sòria-Perpinyà *et al.* (2019b) as follows: from November to the beginning of January, the sluice gates are closed, and the lake water level is about 20 cm above the annual average. The pumps that drain the fields during cultivation are turned off, and the fields below lake level are flooded to encourage the decomposition of organic remains. During January and February, the lake has a higher water renewal rate. Flooded rice fields are pumped empty, water flows out to the sea through Albufera's open sluice gates, and the lake water level also falls. The rice fields remain dry until the beginning of May, when they are reflooded for cultivation. During rice plantation, the sluice gates are partially closed to maintain a mean water flow and mean water level.

Field campaigns

Samples were collected at seven different points within the lake to calibrate the elaborated algorithm and validate the estimated data (Fig. 1). From January 2016 to December 2017, a total of 20 field campaigns were completed, and 114 georeferenced samples were collected. Meteorological information was provided by the Tancat de la Pipa weather station, which is situated close to the lake's northern shore (Fig. 1), and hydrological data was provided by the Jucar Basin Authority (Valencia, Spain). An SD is a standard

Table 1. Spectral information and spatial resolution of MSI Sentinel-2 sensor (ESA, 2012). *Información espectral y resolución espacial del sensor MSI (ESA, 2012).*

Band Number	S2A		S2B		Spatial resolution (m)
	Central wavelength (nm)	Bandwidth (nm)	Central wavelength (nm)	Bandwidth (nm)	
1	443.9	27	442.3	45	60
2	496.6	98	492.1	98	10
3	560.0	45	559	46	10
4	664.5	38	665	39	10
5	703.9	19	703.8	20	20
6	740.2	18	739.1	18	20
7	782.5	28	779.7	28	20
8	835.1	145	833	133	10
8a	864.8	33	864	32	20
9	945.0	26	943.2	27	60
10	1373.5	75	1376.9	76	60
11	1613.7	143	1610.4	141	20
12	2202.4	242	2185.7	238	20

white disc 20 cm in diameter that is submerged vertically until it is no longer visible. The SDD consists of measuring the mean value of the point at which the disc completely disappears and the depth at which it reappears (Wetzel & Likens, 2000). [Chl-*a*] was measured in laboratory using extraction method and its absorbance was measured by a spectrophotometer (Sòria-Perpinyà *et al.*, 2019b).

Remote sensing images

The European Space Agency (ESA) S2 mission is a two-satellite constellation: S2A (launch date: June 23, 2015) and S2B (launch date: March 7, 2017). Each satellite has a sensor called MSI (Multispectral Instrument), which measures Earth's reflected radiance in 13 spectral bands from visible to very-narrow infrared (VNIR) and short-wave infrared (SWIR), with spatial resolutions of 10, 20 and 60 m (ESA, 2012). Table 1 shows the most relevant information about the MSI S2 bands and their corresponding spatial resolutions.

The mission was initially optimized for studies on vegetation, urban planning and terrestrial ecosystems, but the inclusion of new bands

in the *red-edge* (the limit of red and infrared spectral regions), as well as its radiometric quality and high spatial resolution, have proven its usefulness for the study of inland waters (Soria *et al.*, 2017).

Images used in this study were downloaded from the ESA archives, and the dataset consists of S2 A and B imagery. Image processing was completed using SNAP 5 (Brockmann Consult) software. All images were atmospherically corrected by the Sen2Cor processor, which was designed for vegetation and land but also provides good results in eutrophic waters (Soria *et al.*, 2017; Ruescas *et al.*, 2016). A current study of the ESAQS project (Ecological Status of Aquatic Systems with Sentinel Satellites) reinforces the findings above and demonstrates that Sen2Cor results are acceptable for hypertrophic waters. Figure 2 shows part of that study and demonstrates a significant correlation between *in situ* and Sen2Cor reflectance for hypertrophic waters. This result agrees with that observed by Martins *et al.* (2017) for Amazon

dark lakes in the visible bands (Root mean square error RMSE ~ 0.006). This result facilitates the use of already-corrected images provided by ESA for this type of water body.

The images were previously resampled at 20 m with SNAP interpolation tools because the algorithm used in the analysis (described below) uses bands of different spatial resolutions.

Throughout 2016 and 2017, the S2 satellites should have taken 90 images, but were only able to take 81 images in the study area (62 by S2A and 19 by S2B); of these, clouds obscured 39 images, leaving 40 usable images. The time gap between satellite image capture and the field collection campaigns was extended to three days following the methodology of Kutser (2012). For the retrieval algorithm, twenty images were used that were close to the field-collected data: six were coincident, six had a one-day difference, five had two-day differences, and three had three-day differences. SDD differences in eleven samples measured with one- to three-day differences were

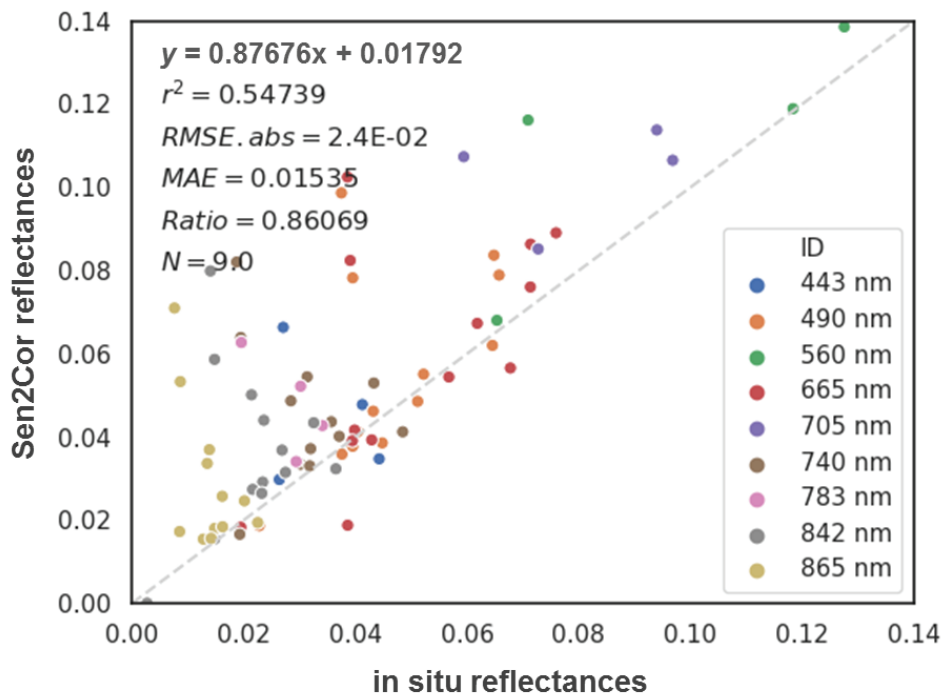


Figure 2. Regression between *in situ* and Sen2Cor reflectances. *Ajuste entre los valores de reflectancia de campo y corregidas con Sen2Cor.*

studied to verify the three-day period; the standard error between pairs was 3.5 % and 1 mm.

Retrieval algorithm

SDD is a measure of water clarity by human eyes (whole visible band), and all optically active substances in the water combine to affect it ([Chl-*a*], chromophoric dissolved organic matter (CDOM) and other substances); therefore, it may be difficult to find conclusive reasons for using some particular wavelengths for retrieval SDD rather than others (Koponen *et al.*, 2002). Our analysis determined the best retrieval algorithm for SDD empirically by a regression model between reflectance values and *in situ* variables, testing three options.

Primarily, a regression was established with Band 3 (537 - 582 nm, *R560*) of the MSI sensor on board the S2. It is nearest to Band 2 (520 - 600 nm) of the TM sensor on board the Landsat 5 satellite, which has been used successfully (Doña *et al.* 2011, 2014), to estimate water transparency by remote sensing in the Albufera study area.

Secondly, a regression was established with a band ratio by using Band 2 (439 - 535 nm, *R495*) like a numerator and Band 5 (694 - 714 nm, *R704*) like a denominator. These MSI bands are the most similar ratios respective to the ratio developed by Koponen *et al.* (2002) using MERIS simulated data, (band 500 - 520) / (band 695 - 715). The ratio developed by Koponen *et al.* (2002) was applied because it was successfully used in a study by Matthews *et al.* (2010) carried out in Zeekoevlei lake (Cape Flats, Cape Town, South Africa) that compared nine algorithms. That lake has limnological conditions similar to those Albufera of València, with a mean [Chl-*a*] of 148.6 ± 8.1 µg/L (with a maximum of 247.4 µg/L and a minimum of 61.0 µg/L) and a mean SDD of only 0.28 ± 0.01 m and similar Mediterranean climatology.

Third, SDD and [Chl-*a*] are inversely related, and some algorithms to obtain [Chl-*a*] have compared the ratio of the reflectance at the peak around 700 nm to the reflectance at the peak around 560 nm, which is related to a minimum in the combined absorption by phytoplankton pigments, particles and CDOM (Gurlin *et al.*,

2011). This inverse ratio was tested using a Band 3 (*R560*) like a numerator and Band 5 (694–714 nm, *R704*) like a denominator.

Data analyses

For calibration and validation of the three algorithms, the 114 data were randomly divided into 79 for calibration and 35 for validation. The three algorithms were calibrated with a linear regression between the georeferenced field data and the reflectance of S2 bands in the same pixel. The algorithms were validated by adjusting a linear regression between the estimated data and field data and calculating the RMSE. The RMSE percentage was calculated using the average of the estimated values. Additionally, Student's t-test was applied to check whether differences between the values provided by the different monitoring points were statistically significant. A boxplot with estimated data of the entire surface of the lake for each image was created to depict the SDD data of the thematic maps, which allow the data dispersion on each map to be seen; variations depending on the SDD in the lake can also be observed.

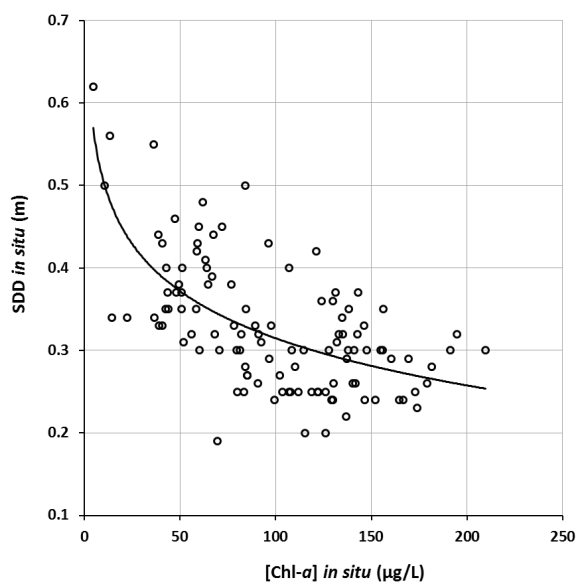


Figure 3. Relationship between SDD and [Chl-*a*]. *Relación entre las medidas de SDD y [Chl-a].*

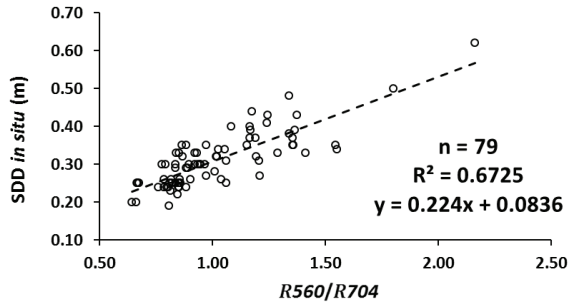


Figure 4. Algorithm calibration. Regression between $R560/R704$ ratio and field data. *Calibración del algoritmo. Regresión entre el cociente $R560/R704$ y los datos de campo.*

RESULTS

Field data

During the two-year study period, a total of 114 samples were collected on 20 different dates. The mean, maximum and minimum values for each sample were measured.

The average value of the SDD results was 0.33 m, ranging between 0.19 m registered at sampling point 3 (lake center, Fig. 1) during June 2017, and 0.62 m registered at sampling point 6 (south lake) during April 2017. These values show the small spatial and temporal variability occurring within the lake. The [Chl-*a*] data shows greater variability, with a maximum value of 209 $\mu\text{g/L}$ recorded in October 2017 at sampling point 2 (north lake) and a minimum value of 4.5 $\mu\text{g/L}$ observed at sampling point 6 (south lake) during April 2017; the average value was 97 $\mu\text{g/L}$. Figure 3 shows that SDD and [Chl-*a*] are inversely related. For these samples, the SDD was principally influenced by [Chl-*a*], which explains 66 % of the total transparency ($r = 0.66$; $p < 0.001$; $n = 114$).

Retrieval algorithm

The established correlations with ratios are in a positive direction for SDD, as larger values indicate less turbid water. Only the correlation with a single band ($R560$) showed an inverse correlation and reached the smallest $R^2 = 0.037$. The band ratio following the Koponen *et al.*

(2002) model and successfully used by Matthews *et al.* (2010) with MERIS was satisfactorily used through the $R560/R704$ ratio with an R^2 of 0.673 (Fig. 4), which was much higher than the R^2 of 0.234 obtained with the $R495/R704$ ratio.

To validate the retrieval algorithm, a linear regression method was used combining the field data and estimated values generated by the algorithm from the S2 images (Fig. 5). An R^2 of 0.748 for a total of 35 samples was obtained, which produces a degree of significance lower than 0.001. However, the fit line indicates that the algorithm tends to underestimate high SDD values. Regarding the calculated errors, the RMSE reached a value of 0.07 m, and the percentage of RMSE was 20 %.

Image output

Applying the algorithm to the S2 images, allowed maps of SDD to be generated that allowed its temporal and spatial evolution to be recorded. As seen in Figure 6, of the 40 images processed for this work, only 14 were significant, those that clearly illustrate changes in SDD. The sequence of images selected shows the annual cycle of

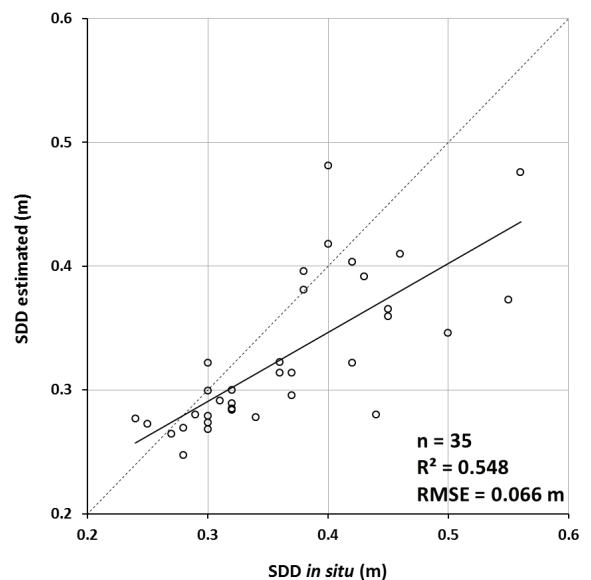


Figure 5. Algorithm validation, observed versus predicted data. *Validación del algoritmo, datos observados frente a estimados.*

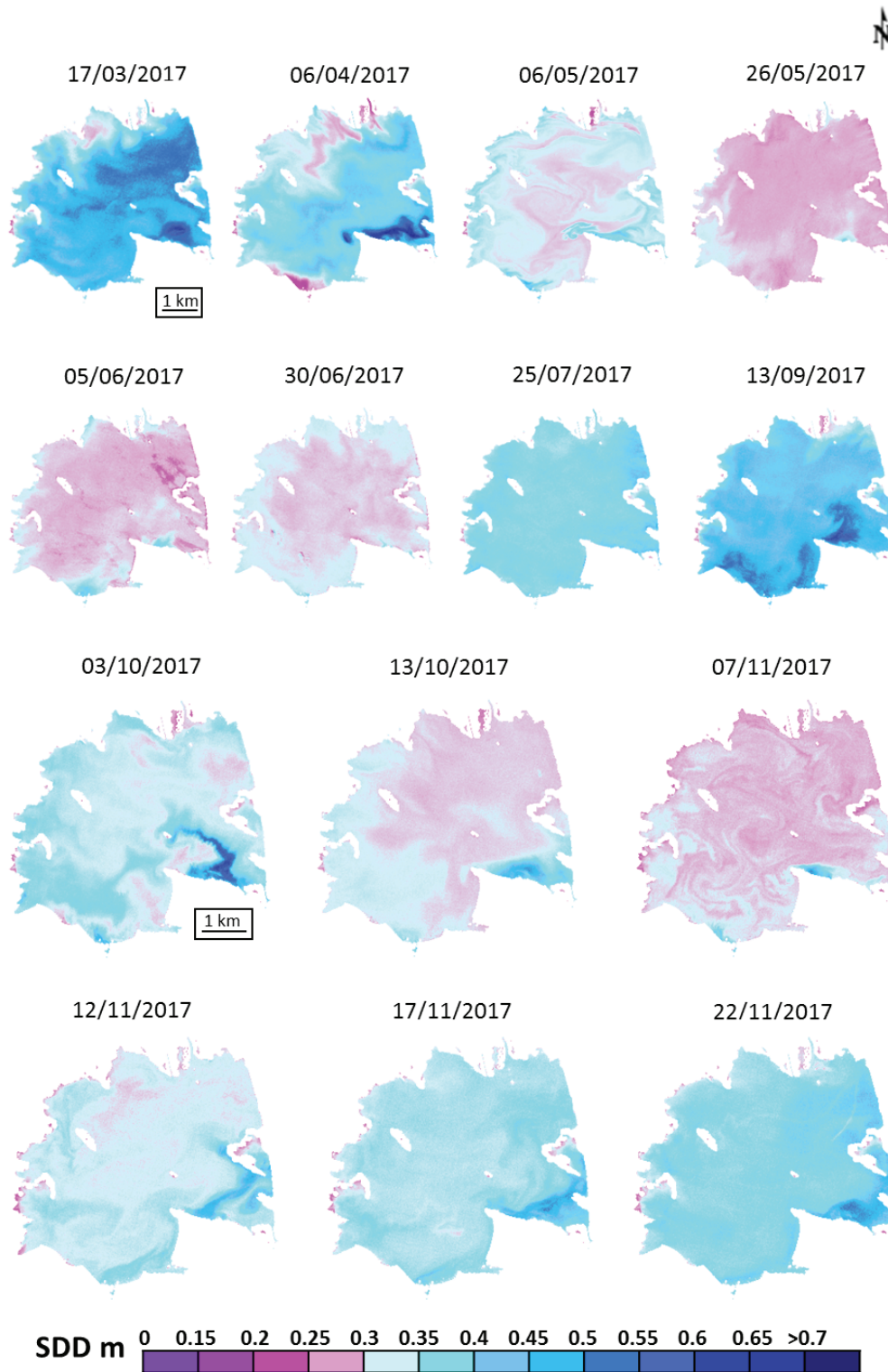


Figure 6. Temporal evolution of SDD in Albufera of València for the year 2017. *Evolución temporal de la SDD en la Albufera de València para el año 2017.*

SDD throughout 2017; this year had more variations than 2016. Images in the first row show the reduction of SDD, from high transparency in March to lowest transparency in late May; SDD reduction begins in the north of the lake, then expands to the south and finally spreads to the east. In the second row, the SDD increases progressively until reaching its highest values at the end of summer. In the third row, a reduction of SDD can be observed starting in the center of the lake and progressing outward toward the shore, until reaching a minimum SDD on November 7. Finally, the last row shows how the SDD increases from the coast toward the center of the lake. Throughout this sequence it is evident that the values of SDD around sampling point 6 (south lake) were consistently much higher than those in the rest of the lake, due to the water intake going through the Overa man-made irrigation canal (Fig. 1); this is true throughout the year except in the summer months. Figure 7 graphically summarizes the SDD data for the entire surface of the lake for the 2017 thematic maps. It shows that the data dispersion is directly proportional to the median; that is, when the lake transparency is greater, the data dispersion is at its highest.

SDD *in situ* vs. SDD estimated

In addition to the linear regression, Figure 8 represents the temporal variation of SDD (*in situ* and estimated) for the two years of study and

demonstrates the accuracy of the algorithm's assessment. Field data are represented by the mean of the SDD values of each sampling, and the estimated data are represented by the mean of the pixels corresponding to the sampling sites for images nearest to the sampling day (Fig. 8A). The data show that both the field and estimated data describe the same SDD variation pattern over the two years.

Figure 8 also plots the SDD values in the field and estimated data for the points located at the north (Fig. 8B) and south (Fig. 8C) of the lake. Those points registered the maximum and minimum SDD values, respectively, and the difference between those SDD values is statistically significant ($t = 2.403$; $p = 0.021$) according to Student's t-test. That result exemplifies the differences between the north-eastern and southern parts of the lake. Figure 8 also depicts how the algorithm responds appropriately to high and low SDD values. However, as the validation fit indicates, high values such as those of the southern point (Fig. 8C) are the most markedly underestimated. Only in some cases of high transparency underestimation is the difference between the *in situ* and estimated values higher than the calculated RMSE of 0.06 m.

The mean for all the SDD estimated values on the entire lake surface for the 40 cloud-free images was calculated in order to produce a more precise representation. To analyze the ecological behavior of the lake, the SDD temporal trend

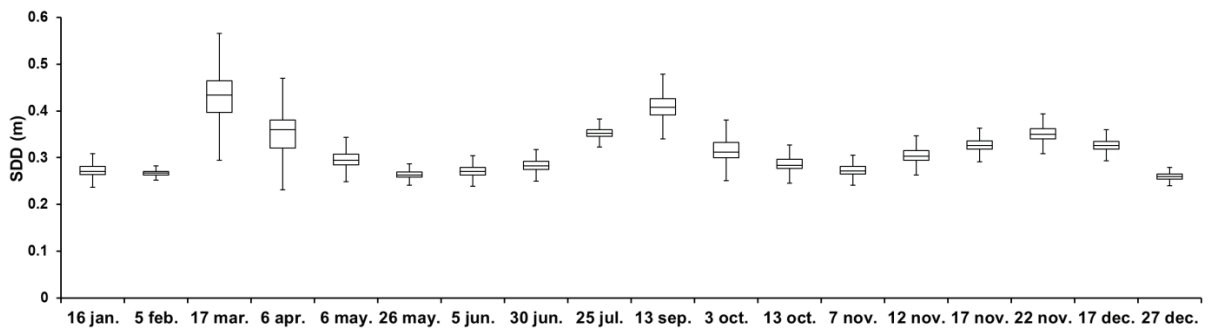


Figure 7. Boxplot of the values range estimated for the images of 2017. For each image, the box bounds the interquartile range (IQR; 25-75 percentile), the horizontal line inside the box indicates the median, and whiskers are $1.5 \cdot \text{IQR}$. Gráfico de cajas del rango de valores estimados para las imágenes de 2017. Para cada imagen, la caja limita el rango intercuartil (IQR; percentil 25-75), la línea horizontal dentro de la caja indica la mediana y los bigotes son el $1.5 \cdot \text{IQR}$.

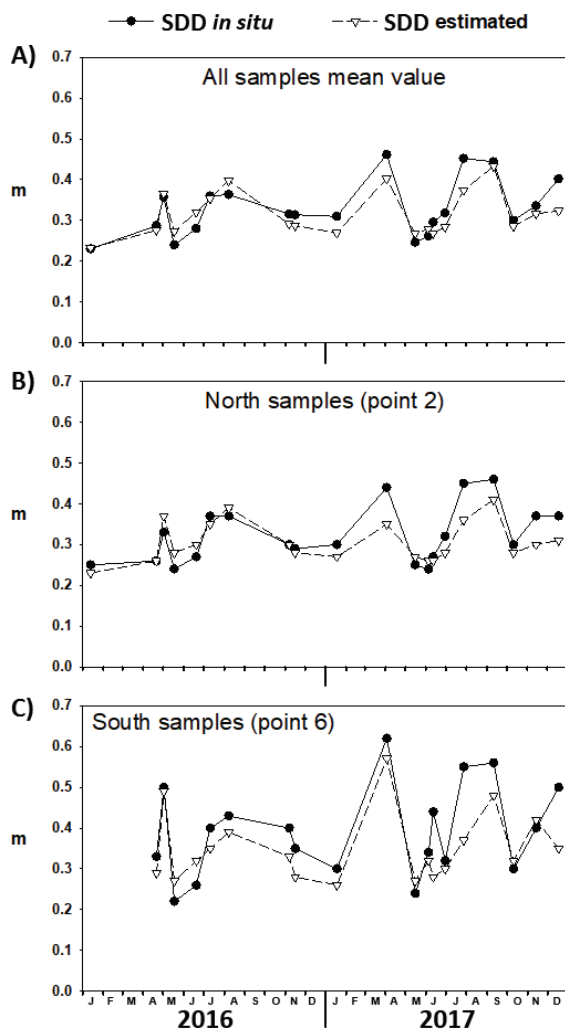


Figure 8. Temporal evolution of *in situ* and estimated SDD, using for the same day the mean of all samples (A) and on the other hand the values of North (B) and South (C) sampling points separately. *Evolució temporal de la SDD in situ y estimada utilizando la media de todas las muestras de un mismo día (A) y por otro lado los valores de los puntos de muestreo Norte (B) y Sur (C) por separado.*

throughout the two-year study could be compared with the other variables obtained. Figure 9 represents the SDD temporal variation coupled with the [Chl-*a*] (estimated values in Sòria-Perpinyà *et al.*, 2019), the monthly water renewal and daily precipitation. The SDD (Fig. 9A) registered two annual maxima, one at the beginning of March and the other at the end of August or the begin-

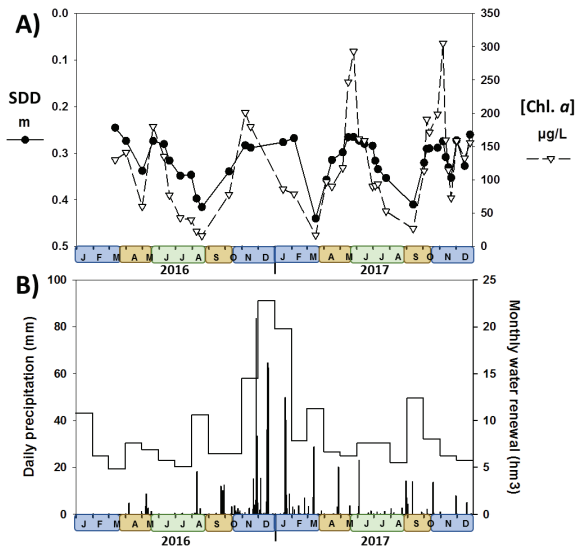


Figure 9. Evolution of SDD and [Chl-*a*] using the mean values on the entire water surface from estimated values (A), hydrological information for water renewal (B-continuous line) and meteorological information for precipitation data (B-bars). Note: blue=flooded fields, brown=dry fields, green=flooded paddies. *Evolució de la SDD y la concentració de clorofila a utilitzant los datos estimados para toda la superficie de agua (A), la información hidrológica para la renovación del agua (B-línea continua) y la información meteorológica para la precipitación (B-barras). Nota: azul=campos inundados, marrón=campos secos, verde=arrozales inundados.*

ning of September. These maxima coincided with the moments of greatest water renewal (Fig. 9B), if the winter period is excluded.

In the [Chl-*a*] variation (Fig. 9A), the peaks with minor values coincide with times of greater transparency. Furthermore, [Chl-*a*] registered two maxima per year, which do not match with the lowest transparency measurements because the lowest SDD values can occur at other moments of the year.

DISCUSSION

The estimated SDD values from the S2 images are possibly due to the accuracy of the retrieval algorithm for Albufera lake, as demonstrated by the calibration and validation results. On the one hand, the determination coefficient of linear regression between the *R560/R704* ratio and the field data was 0.673, very similar to the 0.684

obtained by Matthews *et al.* (2010). Also, the RMSE of 0.06 m is similar to those obtained by Doña *et al.* (2011, 2014); 0.05 m and 0.10, respectively, using the TM2 from a Landsat 5 satellite. The RMSE, the good correlation coefficient between the field and estimated data and the correspondence in the temporal variation between the *in situ* and the estimated data show that the retrieval algorithm strongly matches the results for the Albufera.

A comparison of the thematic maps (Fig. 6) and SDD trend (Fig. 9) reveals that the annual evolution of SDD shows two maxima per year. Anthropogenic action plays a determinative role in water system management of the Albufera lake and can explain the pattern. The first SDD maximum is recorded around March, coinciding with an increase in the lake's water renewal due to inflow water pumped to drain the rice paddies that are intentionally flooded in winter. This event is called the Clear Water Phase and has been described in several studies (e.g., Miracle & Sahuquillo, 2002 and Sòria-Perpinyà *et al.*, 2019b). After several weeks, SDD decreases until the first annual minimum, which occurs at the end of May.

The second maximum occurs at the end of August or the beginning of September; it is facilitated by two factors: (1) an increase in the renewal of the lake's water caused by the draining of rice paddies prior to the harvest period and (2) a decline in primary production, such as the decline in [Chl-*a*], due to nutrient depletion following the typical production peak in late spring (Russel-Hunter, 1970). The second yearly minimum of SDD occurs in November and is due to increased algal growth caused by nutrients entering the system along with rainwater runoff that is used to flood the fields situated below lake level.

This depends greatly on the sampling scheme, but a bimodal pattern arises and is thought to be caused by an assortment of natural and anthropic factors, but especially anthropic ones. An examination of SDD temporal variation depicted in Figure 9 shows that moments of high transparency occur after the fields were emptied, either for tillage or the rice harvest. These periods coincide with increases in water renewal (if periods of heavy rainfall are excluded) and the opening of

the sluice gates, totally or partially, resulting in increased transparency from the shores (water entrance) toward the center and east (the water flows out to the sea). In contrast, the transparency minimums register after the fields have been filled, either for the rice cultivation or the winter dormancy period. In those times, the sluice gates are closed, and water entry provides nutrients that contribute to algal growth and the consequent [Chl-*a*] increase and transparency decrease.

Discrepancies in these overlapping SDD and [Chl-*a*] patterns occur mainly in the winter months, when westerly winds blow strongly (more than 40 km/h) and cause resuspended sediment, producing non-algae turbidity. The absence of submerged macrophytes increases sediment resuspension and consequently enhances water turbidity (Barko & James, 1997; Horppila & Nurminen, 2003). Within this spatial heterogeneity, the SDD help identifies areas of poorer- or better-quality water.

Figure 6 depicts an important entry point of high-quality water at the mouth of the Overa irrigation canal, just south of sampling point 6. In the S2 images, water inflow can be observed as well as the plume that formed within the lake - a feature that would be impossible to discern with field sampling techniques. The plume hydrodynamics generally travel eastward to sea connections, except when hard winds (> 20 km/h) cause the plume to shift to other directions.

The circumstances illustrated in Figure 6 indicate that water inflow through the Overa irrigation canal only renews the south-eastern sector of the lake during an 11-day renovation period (Soria & Vicente, 2002). But if the inflow point moved to the southwest, this high-quality water could enhance the renovation of a sector that has a 53-day renovation period (Soria & Vicente, 2002). In order to improve the trophic state of the lagoon, due to the interconnection between the irrigation canals, this change is possible only, if the water coming from Overa is derived to the Campets irrigation canal and then through the Portet de Sollana canal. Water enters the lake near the Tancat de Milia, a green filter created to reduce nutrients in the water coming out of the Albufera-Sud sewage plant. If the evolution of the SDD is considered with respect

to previous studies, the values are similar, such as the annual cycle of 1985 presented by Soria *et al.* (1987) and the 1998–2006 period studied by Romo *et al.* (2008).

CONCLUSIONS

This study shows that the retrieval algorithm developed to estimate SDD from S2 satellite images is accurate and appropriate to use within a protocol whose main purpose is to monitor the trophic and ecological status of the Albufera of València in near real time. While the results obtained may be dependent on the sampling scheme, an annual bimodal tendency can be deduced from monitoring carried out throughout the study period. SDD fluctuations are determined by water renewal, which is influenced by two factors: (1) the open or closed status of the sluice gates, and (2) the times when the fields are flooded or drained. The main cause of the Albufera's low transparency is high [Chl-*a*]; therefore, efforts to achieve a clear-water state should focus on reducing its primary production.

ACKNOWLEDGEMENTS

We thank the Tancat de la Pipa weather station for providing daily data of precipitation and wind and the Jucar Basin Authority for providing hydrological data. This work has been supported by project GVPROMETEO2016-132 from Generalitat Valenciana, the ESAQS project, one of the first projects to elaborate models by using S2 images started in 2016.

REFERENCES

- BARKO J. W. & W. F. JAMES. 1997. Effects of submerged aquatic macrophytes on nutrient dynamics, sedimentation and resuspension. In: *The structuring role of submerged macrophytes in lakes*. Jeppesen E., Søndergaard Ma, Søndergaard Mo & Christoffersen K. (eds.): 197-214. Springer, New York. USA.
- BATUR, E. & D. MAKTAV. 2019. Assessment of surface water quality by using satellite images fusion based on PCA method in the Lake Gala, Turkey. *IEEE Transactions on Geoscience and Remote Sensing*, 57: 2893-2989. DOI: 10.1109/TGRS.2018.2879024
- BONANSEA, M., M. LEDESMA, C. RODRIGUEZ & L. PINOTTI. 2019. Using new remote sensing satellites for assessing water quality in a reservoir. *Hydrological Sciences Journal*, 64:1, 34-44. DOI: 10.1080/02626667.2018.1552001
- BREZONIK, P., K. D. MENKEN & M. BAUER. 2005. Landsat-based remote sensing of lake water quality characteristics, including chlorophyll and colored dissolved organic matter (CDOM). *Lake and Reservoir Management*, 21 (4): 373-382. DOI: 10.1080/07438140509354442
- DOÑA, C., V. CASELLES, J. M. SÁNCHEZ, A. FERRI & A. CAMACHO. 2011. Herramienta para el estudio del estado de Eutrofización de masas de agua continentales. *Revista de Tele-detección*, 36: 40-50.
- DOÑA, C., J. M. SANCHEZ, V. CASELLES, J. A. DOMÍNGUEZ & A. CAMACHO. 2014. Empirical relationships for monitoring water quality of lakes and reservoirs through multispectral images. *IEEE Journal of Selected Topics in Applied Earth Observations and Remote Sensing*, 7: 1632-1641. DOI: 10.1109/JSTARS.2014.2301295
- EFFLER S. W., R. GELDA, M. G. PERKINS & D. M. O'DONNELL. 2005. Modeling light attenuation, secchi disk, and effects of tripton in Seneca River, New York, USA. *Journal of American Water Resources Association*, 41: 971-984. DOI: 10.1111/j.1752-1688.2005.tb03781.x
- ESA. 2012. Sentinel-2: ESA's Optical High-Resolution Mission for GMES Operational Services. K. Fletcher (ed.). ESA Communications, Noordwijk. The Netherlands. DOI: 10.1016/j.rse.2011.11.026
- ESTEVEZ, F. A. 1998. *Fundamentos de Limnología*. Interciencia. Rio de Janeiro
- FRENCH, R. H., J. J. COOPER & S. VIGG. 1982. Secchi disc relationships. *Journal of American Water Resources Association*, 18 (1): 121-123.
- GHOLIZADEH, M., A. MELESSE & L. REDDI. 2016. A comprehensive review on water quality parameters estimation using remote sens-

- ing techniques. *Sensors*, 16(8): 1298.
- GURLIN, D., A. A. GITELSON & W. J. MOSES. 2011. Remote estimation of chl-*a* concentration in turbid productive waters-Return to a simple two-band NIR-red model? *Remote Sensing of Environment*, 115 (12): 3479-3490.
- HORPPILA, J. & L. NURMINEN. 2003. Effects of submerged macrophytes on sediment resuspension and internal phosphorus loading in Lake Hiidenvesi (southern Finland). *Water Research*, 37 (18): 4468-4474. DOI: 10.1016/S0043-1354(03)00405-6
- IANNUZI, T. J., M. P. WEINSTEIN, K.G. SELLNER & J. G. BARRET. 1996. Habitat disturbance and marine development: An assessment of ecological effects. I. Changes in primary production due to dredging and marine construction. *Estuaries*, 19: 257-271.
- KIRK, J. T. O. 1994. *Light and photosynthesis in aquatic ecosystems*. Cambridge University Press, Cambridge. UK.
- KOPONEN, S., J. PULLIAINEN, K. KALLIO & M. HALLIKAINEN. 2002. Lake water quality classification with airborne hyperspectral spectrometer and simulated MERIS data. *Remote Sensing of Environment*, 79 (1): 51-59. DOI: 10.1016/S0034-4257(01)00238-3
- KUTSER, T. 2012. The possibility of using the Landsat image archive for monitoring long time trends in coloured dissolved organic matter concentration in lake waters. *Remote Sensing of Environment*, 123: 334-338. DOI: 10.1016/j.rse.2012.04.004
- LATHROP, R. G. 1985. *Use of Thematic Mapper data to assess water quality in southern Green Bay and central Lake Michigan*. University of Wisconsin-Madison.
- MARTINS, V. S., C. C. F. BARBOSA, L. A. S. de CARVALHO, D. S. F. JORGE, F. D. L. LOBO & E. M. L. D. M. NOVO. 2017. Assessment of atmospheric correction methods for Sentinel-2 MSI images applied to Amazon floodplain lakes. *Remote Sensing*, 9 (4): 322. DOI: 10.3390/rs9040322
- MATTHEWS, M. W. 2011. A current review of empirical procedures of remote sensing in inland and near-coastal transitional waters. *International Journal of Remote Sensing*, 32 (21), 6855-6899. DOI: 10.1080/01431161.2010.512947
- MATTHEWS, M. W., S. BERNARD & K. WINTER. 2010. Remote sensing of cyanobacteria-dominant algal blooms and water quality parameters in Zeekoevlei, a small hypertrophic lake, using MERIS. *Remote Sensing of Environment*, 114 (9): 2070-2087. DOI: 10.1016/j.rse.2010.04.013
- MIRACLE, M. R. & M. SAHUQUILLO. 2002. Changes of life-history traits and size in *Daphnia magna* during a clear-water phase in a hypertrophic lagoon (Albufera of Valencia, Spain). *Verhandlungen des Internationalen Verein Limnologie*, 28: 1203-1208.
- NAVALGUND, R. R., V. JAYARAMAN & P. S. ROY. 2007. Remote sensing applications: an overview. *Current Science*, 93: 1747-1766.
- ONANDIA, G., A. GUDIMOV, M. R. MIRACLE & G. ARHONDITSIS. 2015. Towards the development of a biogeochemical model for addressing the eutrophication problems in the shallow hypertrophic lagoon of Albufera de Valencia, Spain. *Ecological Informatics*, 26: 70-89. DOI: 10.1016/j.ecoinf.2015.01.004
- OWEN, T. 1985. *Handbook of common methods in limnology*. Kendall/Hunt Publishing Company. IA. U.S.
- PREISENDORFER, R. W. 1986. Secchi disc science. Visual optics of natural waters. *Limnology and Oceanography*, 31: 909-926. DOI: 10.4319/lo.1986.31.5.0909
- RODRIGUES, T., E. ALCÂNTARA, F. WATANABE & N. IMAI. 2017. Retrieval of Secchi disk depth from a reservoir using a semi-analytical scheme. *Remote Sensing of Environment*, 198: 213-228.
- ROMO, S., A. GARCÍA-MURCIA, M. J. VILLENA, V. SÁNCHEZ & A. BALLESTER. 2008. Tendencias del fitoplancton en el lago de la Albufera de Valencia e implicaciones para su ecología, gestión y recuperación. *Limnetica*, 27: 11-28.
- RUESCAS, A. B., M. PEREIRA-SANDOVAL, C. TENJO, A. RUIZ-VERDÚ, F. STEINMETZ & L. DE KEUKELAERE. 2016. Sentinel-2 Atmospheric Correction Intercomparison over two lakes in Spain and Peru-Bolivia. Proceedings of Colour and Light in the

- Ocean from Earth Observation: Relevance and Applications. September 6-8, 2016. Frascati, Rome, Italy.
- RUFFINK, K. 1998. The persistence of anthropogenic turbidity plumes in a shallow water estuary. *Estuarine, Coastal and Shelf Science*, 47: 579-592.
- RUSSEL-HUNTER, W. 1970. *Aquatic productivity: an introduction to some basic concepts of biological oceanography and limnology*. McMillan, NY. USA.
- SCHNEIDER, K. & W. MAUSER. 1996. Processing and accuracy of Landsat Thematic Mapper data for lake surface temperature measurement. *International Journal of Remote Sensing*, 17 (11): 2027-2041.
- SORIA, J. M., M. R. MIRACLE & E. VICENTE. 1987. Aporte de nutrientes y eutrofización de la Albufera de Valencia. *Limnetica*, 3 (2): 227-242.
- SORIA, J. M. & E. VICENTE. 2002. Estudio de los aportes hídricos al parque natural de la Albufera de Valencia. *Limnetica*, 21 (1-2): 105-115.
- SORIA, X., J. DELEGIDO, E. P. URREGO, M. PEREIRA-SANDOVAL, E. VICENTE, A. RUIZ-VERDÚ, J. M. SORIA, R. PEÑA, C. TENJO & J. MORENO. 2017. Validación de algoritmos para la estimación de la clorofila-a con Sentinel-2 en la Albufera de València. Proceedings of the XVII Congreso de la Asociación Española de Teledetección. Octubre 3-7, 2017. Murcia, Spain: 289-292.
- SÒRIA-PERPINYÀ, X., P. URREGO, M. PEREIRA-SANDOVAL, A. RUIZ-VERDÚ, R. PEÑA, J. M. SORIA, J. DELEGIDO, E. VICENTE & J. MORENO. 2019. Monitoring the ecological state of a hypertrophic lake (Albufera of València, Spain) using multitemporal Sentinel-2 images. *Limnetica*, 38 (1): 457-469. DOI: 10.23818/limn.38.26
- SÒRIA-PERPINYÀ, X., M. R. MIRACLE, J. SORIA, J. DELEGIDO & E. VICENTE. 2019b. Remote sensing application for the study of rapid flushing to remediate eutrophication in shallow lagoons (Albufera of Valencia). *Hydrobiologia*, 829: 125-132. DOI: 10.1007/s10750-018-3741-6
- VICENTE, E. & M. R. MIRACLE. 1992. The coastal lagoon Albufera de Valencia: An ecosystem under stress. *Limnetica*, 8: 87-100.
- WANG, P. F., J. MARTIN & G. MORRISON. 1999. Water quality and eutrophication in Tampa Bay, Florida. *Estuarine, Coastal and Shelf Science*, 49: 1-20. DOI: 10.1006/ecss.1999.0490
- WETZEL, R.G. 1975. *Limnology*. W.B. Saunders. Philadelphia. USA.
- WETZEL, R. G. 2001. *Limnology*. W.B. Saunders Co. Philadelphia. USA.
- WETZEL, R. G. & G. E. LIKENS. 2000. Composition and biomass of phytoplankton. In: *Limnological Analyses*. R. G. Wetzel & G. E. Likens (eds.): 147-174. Springer, New York. USA. DOI: 10.1007/978-1-4757-3250-4_10
- WEYL, P. 1970. *Oceanography. An introduction to the marine environment*. John Wiley & Sons, Inc., NY. USA.

Con el patrocinio de:

